CAN’T HIDE FROM *Iris*

iRICELL digital flow morphology automates urine microscopy imaging with direct correlation to the manual method. An extensive image comparison study—conducted by Sorin Gîju, Ph.D., clinical chemist and lead of the Urinary Biochemistry department at Clinical Emergency Hospital Timisoara, Romania—analyzed urine particle images captured by the iRICELL2000 and manual microcopy using filters on the same patient sample. As displayed below, Dr. Gîju’s study shows strong correlation between the two methods.

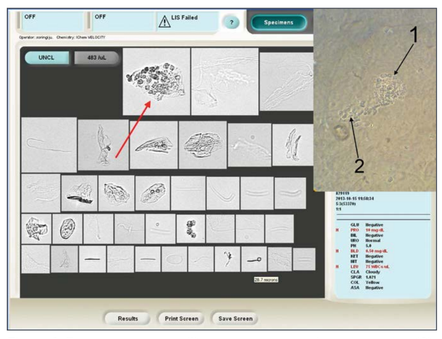

Figure 1: Erythrophagocyte (1) next to dysmorphic erythrocytes (2) isolated from the urinary sediment of a patient with endocapillary proliferative glomerulonephritis. Native preparation. Ph.C.M x 640 (brown-gray filter).

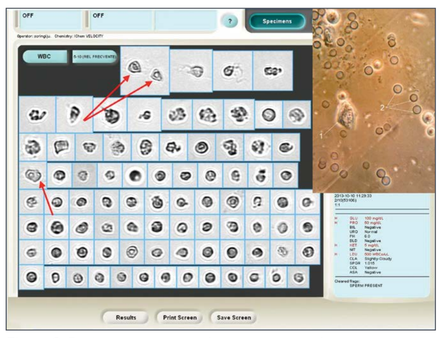

Figure 2: Rectangular renal proximal tubular cell with a large, centrally located nucleus (1) next to red blood cells (2). Native unstained preparation. Ph.C.M x 640 (brown filter).

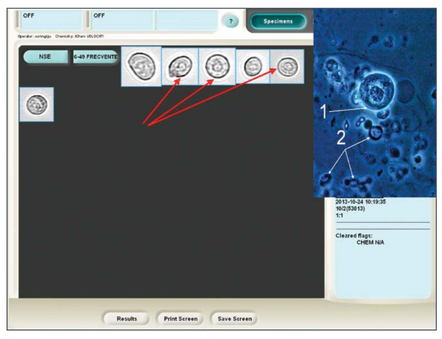

Figure 3: Oval renal tubular cell from the distal convoluted tubules (with a large nucleus, located approximately central, with visible nucleoli) (1) next to dysmorphic red blood cells (acanthocytes) (2). The perinuclear and the cellular halo, which are characteristic for phase contrast microscopy, may be observed. Native unstained preparation. Ph.C.M x 640 (blue filter).

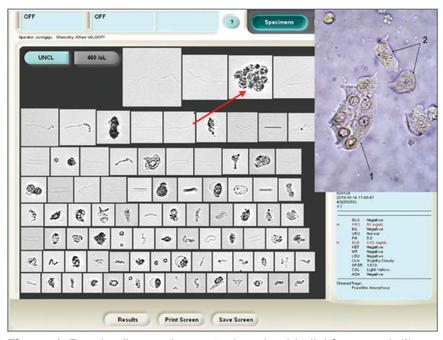

Figure 4: Renal cells conglomerate (renal epithelial fragment) (1) next to proximal renal tubular cells (2). Native unstained preparation. B.F.M x 640.

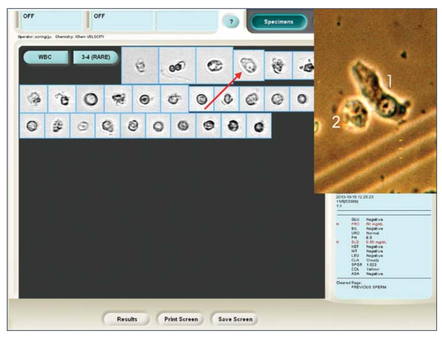

Figure 5: Columnar renal tubular cell with eccentric nucleus and visible nucleolus, originating in the terminal portion of the Bellini’s tubules (1) next to a white blood cell (2). Native unstained preparation. Ph.C.M x 640 (brown filter).

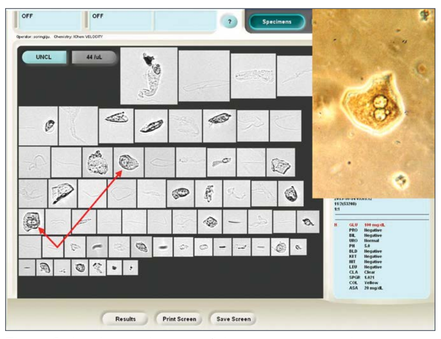

Figure 6: Atypical benign superficial squamous cell, with granular nucleus, detected at the moment of mitosis. Native unstained preparation. Ph.C.M x 640.

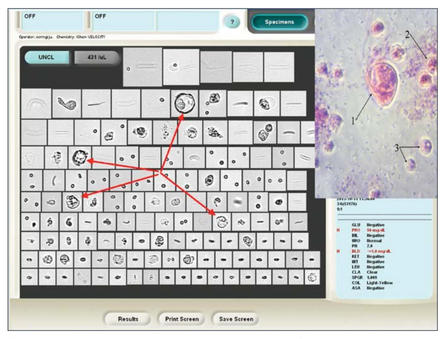

Figure 7: Cell that shows the phenomenon of “cell cannibalism” in a case of urinary bladder transitional cell carcinoma (1), macrophages (2) and polymorphonuclears (3). Sternheimer-Malbin staining. Ph.C.M x 640.

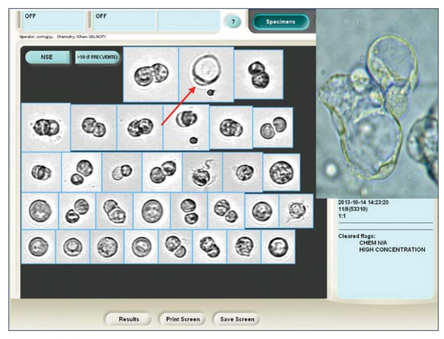

Figure 8: Giant malignant cells with irregular contour and vacuoles observed in the urine sediment of a patient with a tumor of the urinary bladder. It can be observed that the nuclei are compressed towards the periphery. Native unstained preparation. B.F.M x 640.

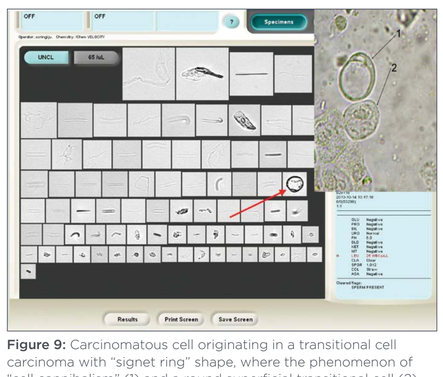

Figure 9: Carcinomatous cell originating in a transitional cell carcinoma with “signet ring” shape, where the phenomenon of “cell cannibalism” (1) and a round superficial transitional cell (2) can be observed. Native unstained preparation. B.F.M x 640.

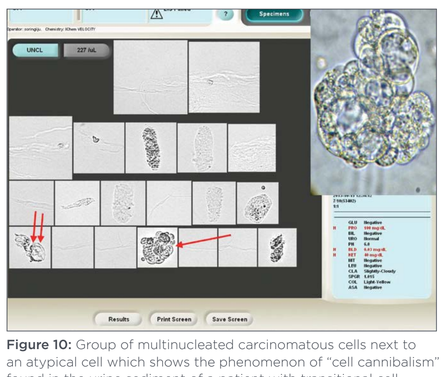

Figure 10: Group of multinucleated carcinomatous cells next to an atypical cell which shows the phenomenon of “cell cannibalism” found in the urine sediment of a patient with transitional cell carcinoma. Native unstained preparation. Ph.C.M x 640.

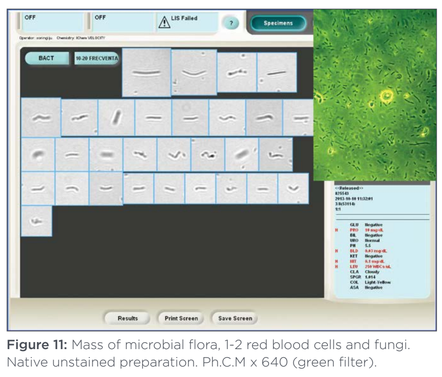

Figure 11: Mass of microbial flora, 1-2 red blood cells and fungi. Native unstained preparation. Ph.C.M x 640 (green filter).

Figure 12: Fungi. Native unstained preparation. B.F.M x 400.

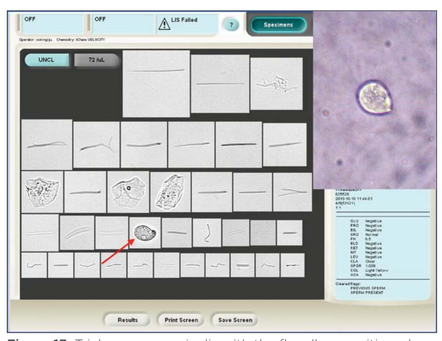

Figure 13: Trichomonas vaginalis with the flagellum positioned on the right side of the body. Native unstained preparation. Ph.C.M x 400.

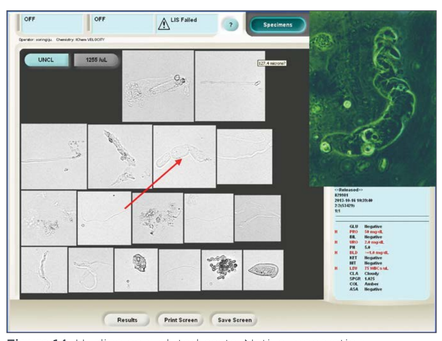

Figure 14: Hyaline convoluted casts. Native preparation. Ph.C.M x 640 (green filter).

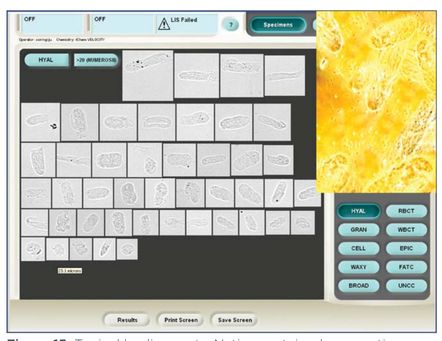

Figure 15: Typical hyaline casts. Native unstained preparation. Ph.C.M x 640.

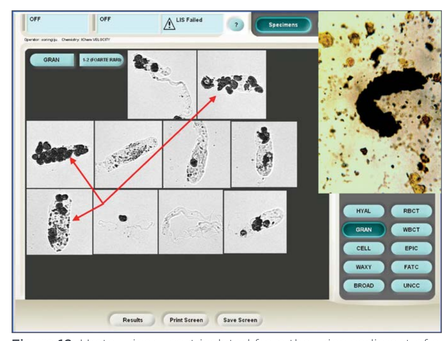

Figure 16: Urate urinary cast isolated from the urine sediment of a patient with gouty nephropathy. Native unstained preparation. B.F.M x 640.

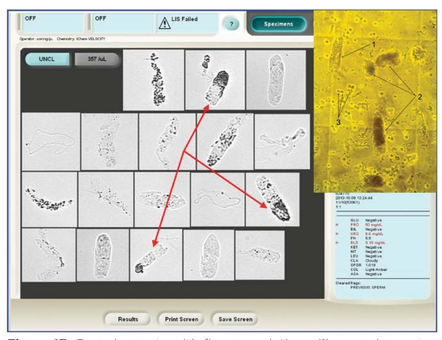

Figure 17: Granular casts with fine granulations (1), granular casts with coarse granulations (2), next to leukocytes (3) and bacterial flora. Native unstained preparation. Ph.C.M x 640 (green filter).

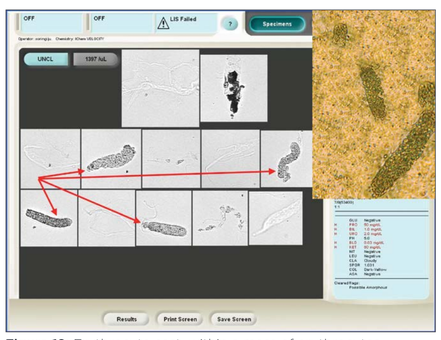

Figure 18: Erythrocyte cast, within a mass of erythrocytes. Native unstained preparation. B.F.M x 400 (brown filter).

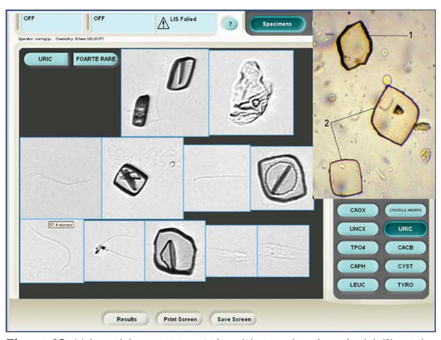

Figure 19: Uric acid macrocrystals with regular rhomboid (1) and irregular rhomboid (2) shapes. Native unstained preparation. Ph.C.M x 640.

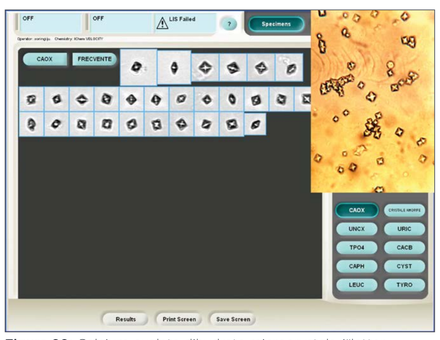

Figure 20: Calcium oxalate dihydrate microcrystals (“letter envelope”). Native unstained preparation. B.F.M x 400 (brown filter).

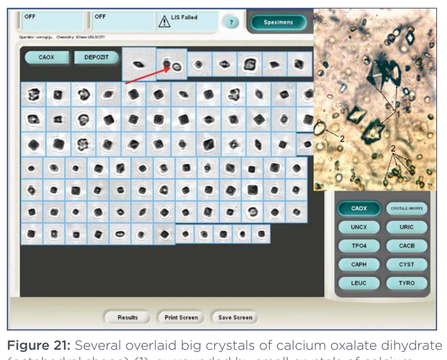

Figure 21: Several overlaid big crystals of calcium oxalate dihydrate (octahedral shape) (1), surrounded by small crystals of calcium oxalate monohydrate (2). Native unstained preparation. B.F.M x 400 (brown filter).

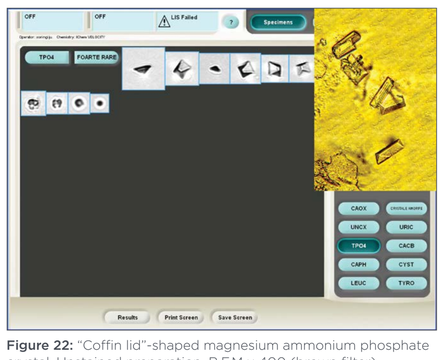

Figure 22: “Coffin lid”-shaped magnesium ammonium phosphate crystal. Unstained preparation. B.F.M x 400 (brown filter).

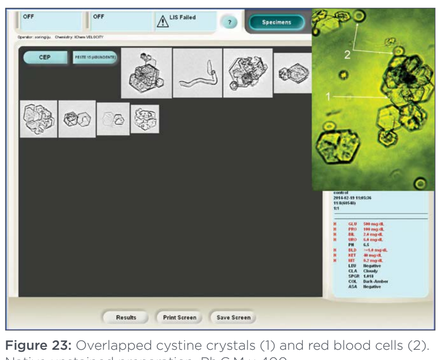

Figure 23: Overlapped cystine crystals (1) and red blood cells (2). Native unstained preparation. Ph.C.M x 400.

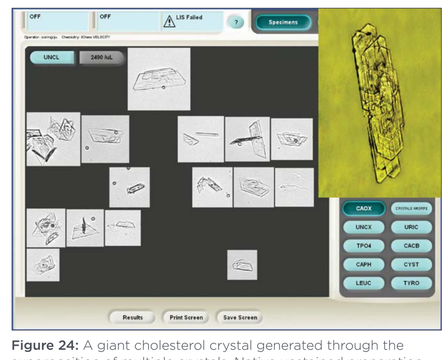

Figure 24: A giant cholesterol crystal generated through the superposition of multiple crystals. Native unstained preparation. B.F.M x 640 (green filter).

All study data and images courtesy of Sorin Gîju, Ph.D., of Clinical Emergency Hospital Timisoara, Romania.

For Beckman Coulter’s worldwide office locations and phone numbers, please visit www.beckmancoulter.com/contact

PO-71183

BECKMAN COULTER | Iris